Global Journal of Engineering and Technology Advances

eISSN: 2582-5003

Cross Ref DOI: 10.30574/gjeta

Journal homepage: https://gjeta.com/

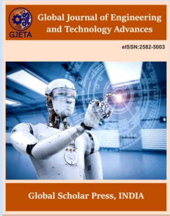

(RESEARCH ARTICLE)

Energy analysis of a simple PV/T system for heating using a variable speed vapor compressor system

Orlando Anaya Reyes [1], Uriel Roberto Gutiérrez Hernández [1], Ignacio Zúñiga González [2], Juan Manuel Belman Flores [2, *] and David Aarón Rodríguez Alejandro [1]

[1] Department of Mechanical Engineering, Engineering Division, Campus Irapuato-Salamanca, University of Guanajuato. Salamanca-Valle de Santiago km 3.5+1.8, C.P. 36885, Mexico.
[2] IRSE Research Group, Department of Mechanical Engineering, Engineering Division, Campus Irapuato-Salamanca, University of Guanajuato. Salamanca-Valle de Santiago km 3.5+1.8, C.P. 36885, Mexico.

Global Journal of Engineering and Technology Advances, 2024, 18(03), 090–101

Publication history: Received on 02 February 2024; revised on 09 March 2024; accepted on 12 March 2024

Article DOI: https://doi.org/10.30574/gjeta.2024.18.3.0044

Abstract

The use of photovoltaic/thermal (PV/T) modules reduces the losses in the photovoltaic cells and, in addition, uses the waste heat in the panel. This paper presents the simulation results of a PV/T system for domestic hot water supply using a vapor compression system during the four seasons of the year in the conditions of Salamanca, Mexico. The results obtained from the simulation indicate that the cooling of the panel causes an increase of approximately 7% in PV efficiency. During the spring, when there is greater solar radiation and, therefore, greater electrical power generation, despite the average temperature of around 36 °C, the lowest efficiency is found. On the other hand, the highest efficiency is achieved in winter, reaching up to 22%. As for the performance coefficient, the highest value is observed during the spring, with a coefficient of performance (COP) of 6.63, while the lowest value is recorded in summer, with a COP of 5.11. It is concluded that this system can satisfy the domestic hot water demand for the conditions under study.

Keywords: Domestic hot-water; Heat pump; Optimization; Photovoltaic energy; Simulation.

1. Introduction

The current situation of the planet is critical as there is a significant risk of triggering irreversible changes if global warming is not limited to below 1.5 °C, as stipulated by the Paris Agreement [1,2]. Based on data from the World Meteorological Organization (WMO), 2023 will be the warmest year on record, data show that the year was about 1.4 °C above the pre-industrial baseline [3]. In the face of this threat, it is vital to urgently address the reduction of carbon emissions. One of the key strategies to achieve this is to reduce energy consumption and transition to cleaner technologies. In this regard, global energy demand is steadily increasing and according to Our World data in 2022, a total of 178,899 TWh will be consumed. Alarmingly, about 80% of this energy came from unsustainable sources, mainly fossil fuels [4].

Since energy demand is increasing year by year and the need to substitute fossil fuels is becoming more and more important, it is of great urgency to develop effective solutions to reduce carbon and greenhouse gas emissions, where solar energy is one of the most promising alternatives towards a more sustainable future [5]. According to data from the International Energy Agency (IEA), by 2022 the installed PV capacity worldwide reached approximately 1185 GW, with a remarkable reduction of 1399 $MtCO_2$ [6]. Despite significant advances, PV technology presents challenges that require attention to maximize its efficiency and effectiveness. Its efficiency is affected by several factors such as soiling, orientation, radiation, and the temperature to which it is exposed. In addition, it is only capable of transforming visible

* Corresponding author: Juan Manuel Belman Flores

light into electricity, while infrared light is converted into thermal energy, thus affecting its performance [7]. In the constant search to increase the efficiency of photovoltaic (PV) cells, attention has been focused on innovative strategies to cool the surface of the cells and take advantage of the waste heat, since it has been proven that the efficiency of the electrical generation of solar cells decreases with increasing temperature. A composite system such as photovoltaic/thermal (PV/T) which applies cooling to the solar cells counteracts this limitation by reducing their operating temperature and utilizing the thermal energy captured in the process. One of the solutions highlighted in recent research is the use of heat pumps, which not only dissipate heat from the panels to improve their efficiency, but also have the potential to provide additional heating. Moreover, it is believed that these devices are capable of meeting 10% of the heating needs of today's buildings [8]. The interest and adoption of heat pumps are on the rise; according to IEA data, sales of heat pumps are expected to grow by 11% by 2022 [8]. Furthermore, the IEA estimates that by 2030 heat pumps could reduce global CO_2 emissions by at least 500 million tons [9].

A heat pump is an efficient technology that can significantly reduce primary energy consumption by recycling waste heat or other low-grade thermal heat. In that sense, the integration of a heat pump with solar technology can be very beneficial. For example, Wang et al. [10] designed and built a solar photovoltaic/thermal heat pump system capable of supplying the electrical demand, providing air conditioning in both winter and summer and hot water all year round, achieving coefficient of operation (COP) values of up to 3.18 in heating mode. Del Amo et al. [11] simulated and experimentally validated a heat pump assisted by thermal photovoltaic panels, obtaining values between 10-22 °C for the cold temperature and a COP of 4.62. Zhou et al. [12] tested a solar-assisted indirect expansion system, and experimentally found electrical, thermal, and overall efficiencies of 15.9%, 33.4%, and 49.3%, respectively, and a COP of 4.7. Liu et al [13] also conducted a study to evaluate the energy, economic and environmental performance of a direct expansion photovoltaic-thermal heat pump system for domestic hot water supply. Their results showed that the proposed system had a 9.67% increase in annual electricity production over traditional PV systems. The system also had a significantly lower environmental impact than conventional heating systems, with a life-cycle environmental impact of only 3-5% compared to electric boilers. Ammar et al [14] simulated and experimentally validated a solar-assisted photovoltaic/thermal heat pump using R134a as the working fluid and a constant-speed Copeland compressor. They developed mathematical models to predict the energy and exergy performance for fixed temperatures of 28 °C, the results showed that the COP increased with solar irradiance.

In this work, the theoretical simulation of a simple PV/T system is proposed, where the refrigeration system or heat pump is integrated by a variable-speed compressor. The simulation is based on the development of a model composed of physical fundamentals and correlations. The paper is organized as follows; section 2 shows a general description of the system, providing information about the most important components and operating conditions; in addition, the methodology used for the analysis and optimization of the vapor compression refrigeration cycle is described. Section 3 shows the discussion of the most relevant results and, finally, section 4 presents the conclusions of the work.

2. Material and methods

2.1. System description

The system under analysis is shown in Figure 1. It consists of a vapor compression cycle working with R1234yf, and uses a photovoltaic panel as an evaporator, taking advantage of the refrigerant as a means of cooling the panel to increase its electrical efficiency. On the other hand, the condenser consists of a coil, through which flows the refrigerant that is inside a tank with water that acts as a secondary fluid. In this way, domestic hot water is produced for domestic use, thanks to the energy it absorbs from the refrigerant. When the pump switches to cold mode, the direction of the cycle is reversed by using a four-way reversible valve. In this mode, the water tank now functions as the evaporator, while, on the condenser side, a magnetic valve closes the passage to the panel, where another opens the passage to a finned heat exchanger that takes advantage of the air temperature to condense the refrigerant. The main characteristics of the pump are shown in Tables 1 and 2, which correspond to the manufacturer's catalog.

Table 1 Main features of the photovoltaic panel

Parameter	Value	Units
Surface	4.385	m^2
Maximum Power	450	W
Module Efficiency	20.4	%
Operating Temperature	-40 to 85	$°C$

2.2. Considerations

For the study of this system, a model based on the combination of physical fundamentals, empirical correlations and data provided in the manufacturers' catalogs is presented. To perform a correct analysis, it is necessary to take into account the following considerations:

- The system operates under steady-state conditions.
- Changes in kinetic and potential energy are negligible.
- There are no pressure losses through the piping and heat exchangers.
- The condensing temperature for the simulation is 54 °C.
- The evaporation temperature for the simulation is 12 °C.
- The analysis is carried out under the average meteorological conditions of the city of Salamanca, Mexico.

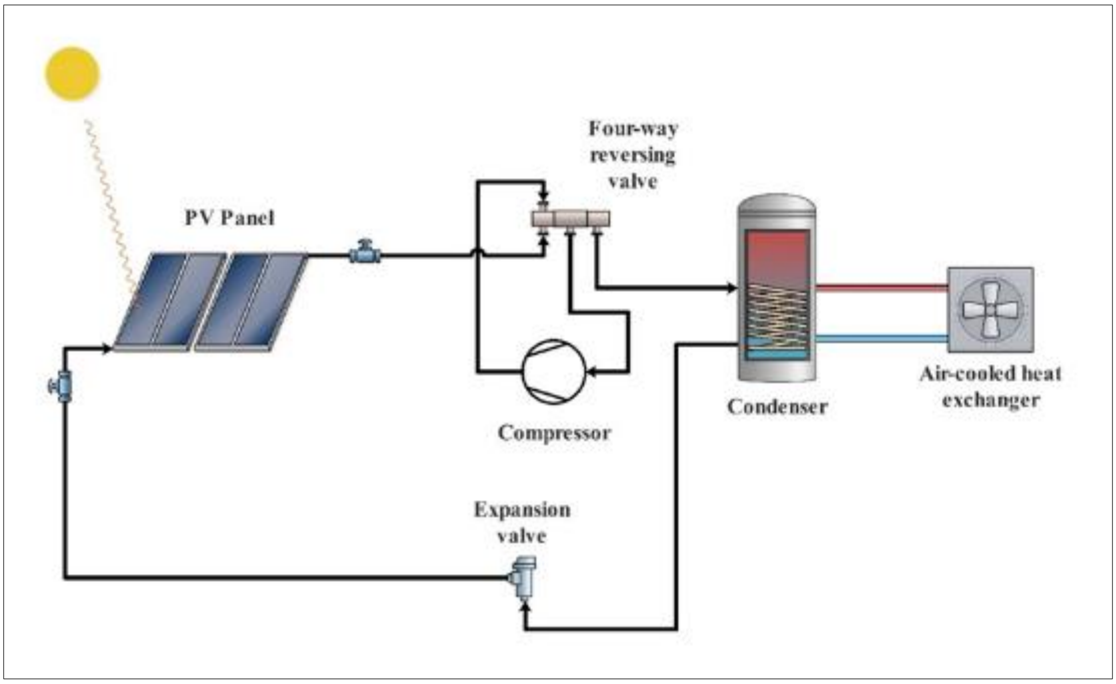

Figure 1 Representative diagram of the system under study

2.3. Physical model

Compressor: For the characterization of the compressor, mass and energy balances are applied, together with an empirical correlation for the developed power provided by the manufacturer. Also, the expression is shown to predict the refrigerant mass flow rate based on the volumetric efficiency of the compressor.

$$\dot{W}_{comp} = \dot{m}_{ref}(h_o - h_i) \qquad ....(1)$$

Table 2 Main features of the photovoltaic compressor

Parameter	**Value**	**Units**
Maximum discharge temperature	130	$°C$
Maximum compression ratio	8:1	-
Compressor rotation speed	3200-5700	rpm
Volumetric displacement	16.1	cm^3

$$\dot{W}_{comp} = C_1 + C_2N + C_3N^2 + C_4N^3 + C_5T_{evap} + C_6T_{evap}^2 + C_7T_{evap}^3 + C_8T_{cond} + C_9T_{cond}^2 + C_{10}T_{cond}^3 + C_{11}NT_{cond}T_{evap} + C_{12}N^2T_{cond}T_{evap} + C_{13}NT_{evap}^2T_{cond} + C_{14}NT_{evap}T_{cond}^2 + C_{15}NT_{evap} + C_{16}NT_{cond} + C_{17}T_{evap}T_{cond} + C_{18}N^2T_{evap} + C_{19}NT_{evap}^2 + C_{20}N^2T_{cond} + C_{21}NT_{cond}^2 + C_{22}T_{cond}^2T_{cond} + C_{23}T_{evap}T_{cond}^2 \quad \ldots\ldots\ldots\ldots..(2)$$

$$\dot{m}_{ref} = \frac{\eta_{vol}V_{disp}N}{v_{suc}} \quad \ldots\ldots\ldots\ldots(3)$$

Where "N" is the compressor rotational speed, ho and hi are the enthalpy at the compressor outlet and inlet, respectively, η_{vol} is the volumetric efficiency, while T_{evap} and T_{cond} are the evaporating and condensing temperatures, respectively. The values of the coefficients can be seen in Table 3. On the other hand, the compression ratio is defined as:

$$CR = \frac{P_{suc}}{P_{desc}} \ldots\ldots\ldots\ldots\ldots..(4)$$

Where "P_{suc}" is the suction pressure at the compressor inlet and "P_{desc}" is the discharge pressure at the compressor outlet. Similarly, for the analysis of the compressor is considered a polytropic process, defined by the following equation:

$$\frac{T_{desc}}{T_{desc}} = \frac{P_{desc}}{P_{suc}}^{\frac{\gamma-1}{\gamma}} \ldots\ldots\ldots\ldots\ldots..(5)$$

Where γ is the specific heats ratio.

$$\gamma = \frac{C_p}{C_v} \ldots\ldots\ldots\ldots\ldots..(6)$$

Evaporator: A photovoltaic panel is used as evaporator, whose specifications can be seen in Table 1. The electrical efficiency of this device (7) will depend on the surface temperature of the T_{PV} panel [15].

$$\eta_{PV} = \eta_r\left[1 - \mu_{PV}\left(T_{PV} - T_{ref}\right)\right] \ldots\ldots\ldots\ldots..(7)$$

Where "μ_{PV}" is the percentage of electrical loss per degree of temperature, and T_{ref} is a reference temperature according to the manufacturer (ambient temperature). Similarly, the energy balance used in this device, taking into account the considerations, the energy absorbed by the panel is dissipated by the coolant flow, where A_s is the surface area of the panel, "G" is the solar irradiance and α is the absorptivity of the panel.

$$\dot{Q}_{PV} = A_s G \alpha \qquad \text{……………..(8)}$$

$$\dot{Q}_{PV} = \dot{m}_{ref}(h_o - h_i) \qquad \text{…………..(9)}$$

Condenser: A water storage tank with a capacity of 200 L functions as the condenser of the system having as operating temperatures of 20 °C at the inlet, likewise, an average specific heat was calculated between both temperature values. Performing an energy balance between both fluids (refrigerant and water) we have:

$$\dot{Q}_{cond} = \dot{m}_{ref}(h_i - h_o) \qquad \text{……………………(10)}$$

$$\dot{Q}_{cond} = \dot{m}_w C_{pw}\left(T_{w,i} - T_{w,o}\right) \qquad \text{……………(11)}$$

Table 3 Coefficients for the correlation of compressor power

Coefficient	Value
C_1	-2.108123e+03
C_2	7.179658e-01
C_3	-1.369964e-04
C_4	1.377041e-08
C_5	-1.402373e+01
C_6	-2.065626e-02
C_7	1.330498e-04
C_8	3.645531e+01
C_9	-3.067540e+01
C_{10}	7.649559e-04
C_{11}	-.164955e-05
C_{12}	8.031881e-09
C_{13}	2.106998e-07
C_{14}	-1.971391e-07
C_{15}	5.009996e-03
C_{16}	-1.785419e-03
C_{17}	9.828440e-02
C_{18}	-7.679661e-07
C_{19}	-2.677387e-05
C_{20}	-1.959383e-07
C_{21}	1.902781e-05
C_{22}	3.644365e-05
C_{23}	2.006717e-04

Expansion valve: Finally, since the expansion valve is adiabatic, the change in internal energy is equal to the work of flow, however, given the definition of enthalpy:

$$h=U+pV \ldots\ldots\ldots\ldots\ldots (12)$$

An isoentalpic process is reached in this device:

$$h_i=h_o \ldots\ldots\ldots (13)$$

2.4. Optimization

In the previous section, the basic model that characterizes the system under study was defined. To extend the analysis, it is proposed to optimize the COP by maximizing this objective function. For this purpose, it has been chosen to use a genetic algorithm (Figure 2), available in the EES software. This process is carried out in compliance with the constraints of the mass and energy balances.

The algorithm works as follows: input parameters are entered (Table 4), then random solutions are generated and, finally, the results that prove to be the most suitable for maximizing the COP are selected.

$$COP = \frac{\dot{Q}_{cond}}{\dot{W}_{comp}} \ldots\ldots\ldots\ldots\ldots\ldots (14)$$

Table 4 Limits of the decision variables according to the ranges of the equipment provided by the manufacturer

Parameter	**Lower bound**	**Upper bound**
Evaporation temperature	-23.3 *℃*	12.8 *℃*
Condensation temperature	26.7 *℃*	65.6 *℃*
Mass flow of water	0.02 *kg/s*	0.07 *kg/s*
Rotation speed	3200 *rpm*	5700 *rpm*

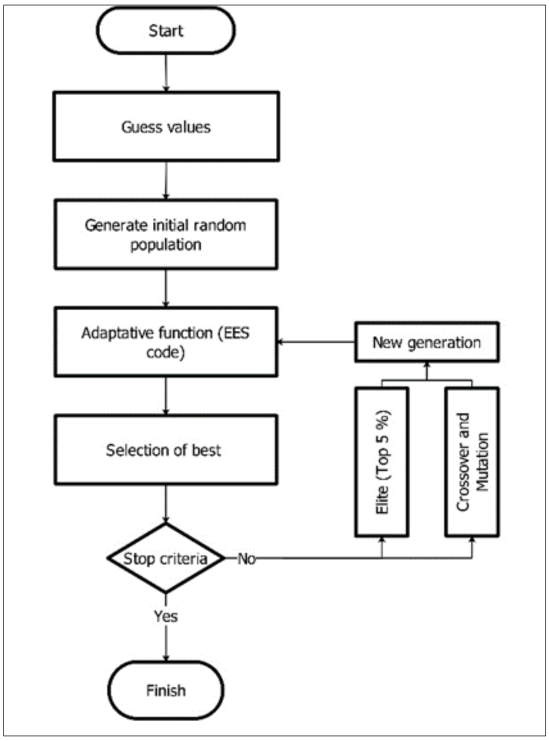

Figure 2 Flowchart for the genetic algorithm used

3. Result and Discussion

The evaluation of the system performance was carried out according to the average meteorological data in the city of Salamanca, Mexico, provided by the National Renewable Energy Laboratory (NREL) of the United States, for the most representative months of the four seasons of the year: April (spring), July (summer), October (fall), January (winter), between 9:00 and 17:00 hours. To validate in some way, the developed model, the theoretical behavior of the heat collection power of the photovoltaic panel obtained in the present work is compared with the experimental behavior reported by Du et al. [16], both analyzed during the winter season (see Figure 3). It is observed that in both cases, the heat uptake power follows a similar trend, decreasing as the time-of-day progresses. The difference in the order of magnitude of this power is mainly due to the unequal surface areas of the panels in both works.

Figure 4 shows the variation of the water outlet temperature as a function of the time of day. To be considered as domestic hot water suitable for human use, several international standards recommend temperatures between 30 and 45 °C, for example, the Spanish Technical Building Code (CTE) standard [17]. It can be observed that, for all seasons of the year, in the entire range of hours evaluated, these temperatures are met. During the spring, which is the warmest season, the highest temperatures are reached, obtaining maximum values of around 38 °C between 10:00 and 11:00 am. On the other hand, during the summer there is a low solar irradiation and, therefore, the temperatures reached are lower, between 32 and 34 °C. For the autumn, it is observed that a practically constant temperature is maintained between 10:00 and 15:00 hours.

In Figure 5 it is observed how the electrical efficiency of the photovoltaic panel varies as a function of the time of day, during the four seasons of the year, depending on whether or not the panel is cooled by the refrigerant, the continuous and dotted lines indicate the behavior of the efficiency with and without cooling, respectively, with the cooling of the panel having a significant effect on its efficiency. For the spring case, the electrical efficiency of the panel manages to increase by about 7%. It is also observed that the maximum electrical efficiency is reached during the winter because, in addition to the cooling of the panel, the low temperatures of the environment in this season contribute to a further decrease in the temperature of the panel. Thus, it is proven that the cooling of the panel has a significant effect on its performance.

Figure 6 shows the electrical power generated by the panel, depending on the time of the day, varying between 300 and 750 Watts. It is observed that the behavior of this power is like that of the domestic hot water temperature, during the four seasons of the year.

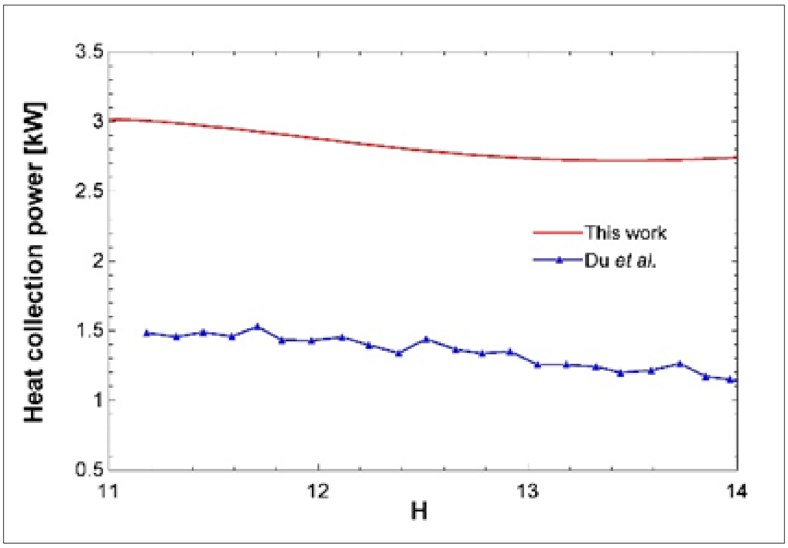

Figure 3 Comparison between the present model and the experimental work of Du et al

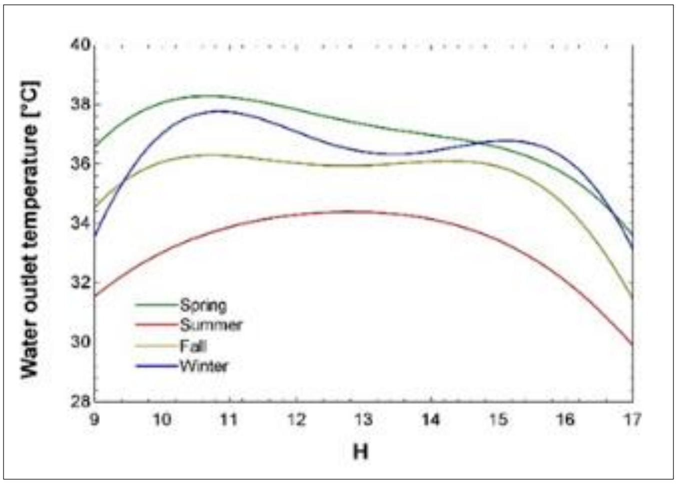

Figure 4 Variation of the water outlet temperature in function of time of day

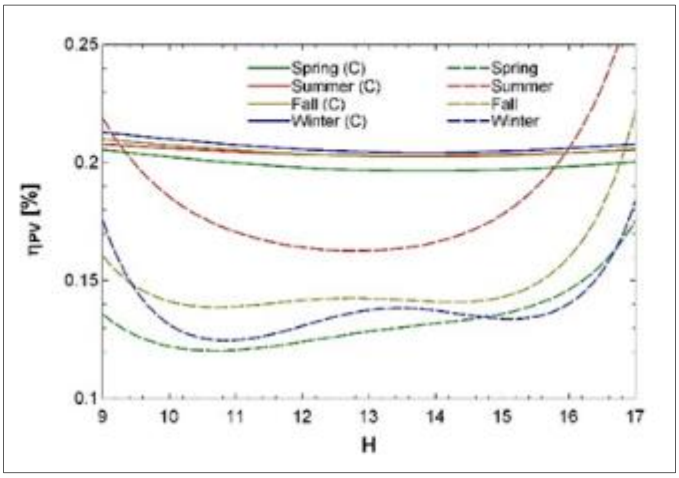

Figure 5 Variation of the electrical efficiency of the panel depending on the time of day with and without cooling

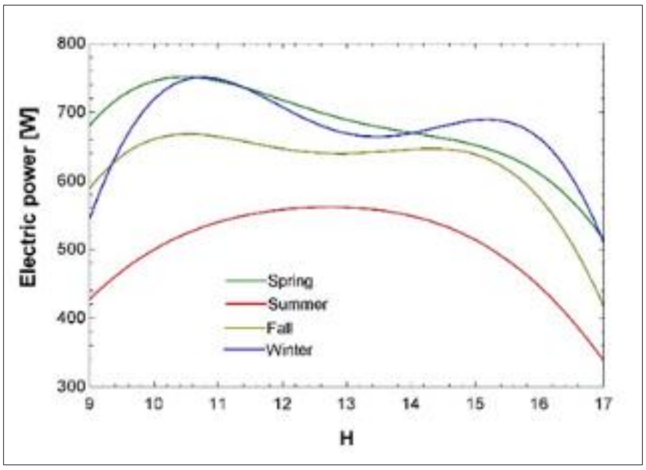

Figure 6 Variation of the electrical power of the panel depending on the time of day

Finally, Figure 7 shows the influence that have the speed of rotation of the compressor operating in the ranges provided by the manufacturer, as the time of day, in the performance coefficient of the system. For the four seasons of the year, the maximum performance coefficients are reached at low speeds of compressor rotation, decreasing as it increases, mainly due to the higher energy consumption required by the compressor to maintain these speeds. On the other hand, the time of day has a more significant influence, following a behavior similar to that presented by the water temperature, sticking to the intensity of solar irradiation during the four seasons. During spring, the maximum COP corresponds to around 5.2, which is reached around midday, while during winter it is 5.05, around 13:00 hours. At low compressor rotation speeds, the time of day does not have a significant impact, so the rotation speed is the parameter that has the greatest influence on the performance of the system.

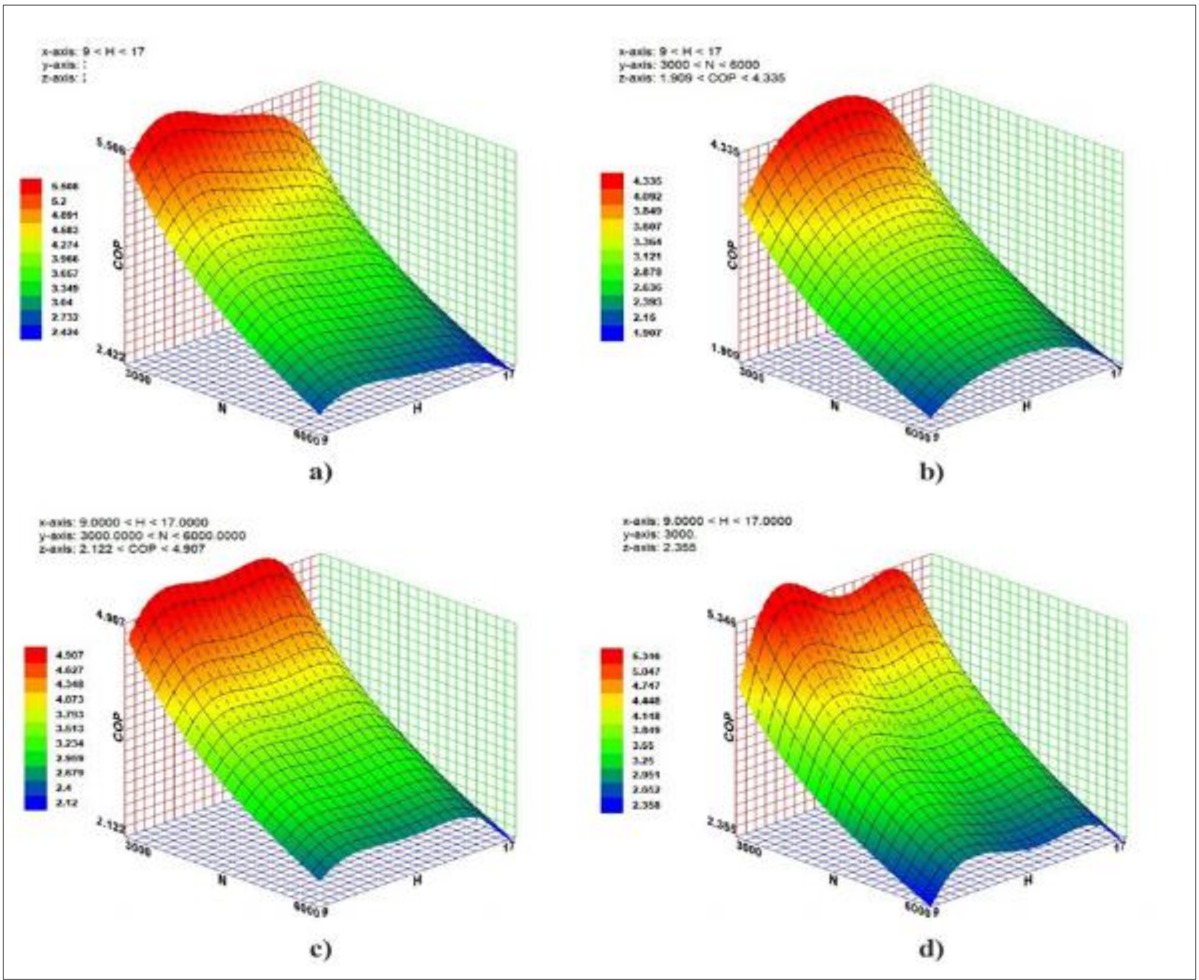

Figure 7 Variation of the COP as a function of the time of day and the rotation speed of the compressor; a) Spring, b) Summer, c) Autumn and d) Winter

3.1. Conditions for optimum COP

Table 5 shows both the original parameters and the parameters found to achieve the optimal COP for each season of the year after maximizing Equation 14. The best conditions for spring were found after 8378 iterations, at generation 107 of 128, with a refrigerant mass flow rate of 0.0249 kg/s, a spin speed of 3208 rpm, a condensing temperature of 45.31 °C and an evaporating temperature of 5.086 °C, observing an increase in COP of 1.12%, being the highest of the four seasons. For the summer, the refrigerant mass flow with which the optimum COP is achieved was 0.0195 kg/s, with a rotational speed of 3206 rpm, a condensing temperature of 45.81 °C and an evaporating temperature of 5.367 °C, increasing the COP by 0. 78%, while for the fall consists of a refrigerant mass flow rate of 0.0221 kg/s, a rotational speed of 3200 rpm, a condensing temperature of 45.35 °C and an evaporating temperature of 6.032 °C, with an increase of 0.96% in COP.

Table 5 Optimization results

Variable	Initial value	Optimized value
Spring		
COP	5.51	6.63
η_{vol}	19.88 %	22.79 %
$T_{w,o}$	38.28 °C	37.62 °C
Summer		
COP	4.33	5.11
η_{vol}	15.64 %	17.67 %
$T_{w,o}$	34.38 °C	33.75 °C
Autumn		
COP	4.90	5.86
η_{vol}	17.69 %	19.63 %
$T_{w,o}$	36.27 °C	35.61 °C
Winter		
COP	5.35	6.45
η_{vol}	19.31 %	22.19 %
$T_{w,o}$	37.76 °C	37.09 °C

Finally, for the winter, the optimum COP was achieved with a refrigerant mass flow rate of 0.0242 kg/s, a rotational speed of 3200 rpm, a condensing temperature of 45.3 °C and an evaporating temperature of 5.021 °C, increasing the COP by 1.1%. Similarly, the values of the volumetric efficiency of the compressor and the water outlet temperature are also shown. In all cases, it is observed that the volumetric efficiency increases, while the water outlet temperature decreases slightly.

Nomenclature

A:	Area (m^2)
C:	Compressor constant
COP:	Performance coefficient
C_P:	Specific heat at constant pressure (kJ/kgK)
C_V:	Specific heat at constant volume (kJ/kgK)
CR:	Compression ratio
H:	Time of the day *(hr)*
H:	Enthalpy *(kJ/kg)*
G:	Solar irradiation
N:	Compressor rotation speed *(rpm)*
$\dot{Q}$:	Heat transfer *(W)*
$\dot{m}$:	Mass flow *(kg/hr)*
T:	Temperature *(°C)*

P: Pressure *(kPa)*

U: Internal energy *(kJ)*

V: Volume *(m^3)*

Greek letters

η: Efficiency *(%)*

α: Panel absorptivity *(-)*

Subscripts

0: Environment condition

1-23: Compressor constants

c,i: Compressor inlet

Cond: Condenser

desc,c: Compressor discharge

Disp: Displacement

Evap: Evaporator

Pv: Photovoltaics

Ref: Cooled

S: Panel surface

Suc: Compressor suction

w,i: Hot water inlet

w,o: Hot water outlet

4. Conclusion

A model combining physical fundamentals, empirical correlations, and data provided by the manufacturer was presented to simulate the behavior of a PV/T system to produce domestic hot water and/or heating.

The system was simulated for environmental conditions during the four seasons of the year in the city of Salamanca, Mexico, to evaluate its performance. The results show how the electrical efficiency of the solar cells increases between 4 and 5 % when a flow of refrigerant is circulated below the surface of the panel, causing a decrease in the surface temperature while acting as an evaporator of the system.

From the point of view of the environmental conditions, both the performance coefficient and the electrical efficiency are mainly influenced by the ambient temperature, since the higher the outside temperature, the higher the surface temperature of the panel, causing a decrease in the electrical efficiency of the panel. As a result, this coupled system is suitable for obtaining domestic hot water practically all year round.

Compliance with ethical standards

Disclosure of conflict of interest

No conflict of interest to be disclosed.

References

[1] United Nations. The paris agreement.

[2] David I. Armstrong McKay, Arie Staal, Jesse F. Abrams, Ricarda Winkelmann, Boris Sakschewski, Sina Loriani, Ingo Fetzer, Sarah E. Cornell, Johan Rockstr¨om, andTimothy M. Lenton. Exceeding 1.5°c global warmingcould trigger multiple climate tipping points. Science,377(6611):eabn7950, 2022.

[3] Mustapha A. Obalanlege, Yasser Mahmoudi, Roy Douglas, Ehsan Ebrahimnia-Bajestan, John Davidson, and David Bailie. Performance assessment of a hybrid photovoltaic-thermal and heat pump system for solar heating and electricity. Renewable Energy, 148:558–572, 2020.

[4] Hannah Ritchie, Pablo Rosado, and Max Roser. Energy. Our World in Data, 2023.

[5] Jie Ji, Hanfeng He, Tintai Chow, Gang Pei, Wei He, and Keliang Liu. Distributed dynamic modeling and experimental study of pv evaporator in a pv/t solar-assisted heat pump. International Journal of Heat and Mass Transfer, 52(5):1365–1373,2009.

[6] EA. Snapshot of global pv markets 2023. Technical Report, Report IEA-PVPS T1-44:2023, IEA. International Energy Agency, Paris, Francia, 2023.

[7] Soowon Chae, Sangmu Bae, and Yujin Nam. Economic and environmental analysis of the optimum design for the integrated system with air source heat pump and pvt. Case Studies in Thermal Engineering, 48:103142, 2023.

[8] Yannick Monschauer, Chiara Delmastro and Rafael Martinez Gordon. Global heat pump sales continue double-digit growth.

[9] IEA. The future of heat pumps. Technical report, IEA. International Energy Agency, Paris, Francia, 2022.

[10] Gang Wang, Yaohua Zhao, Zhenhua Quan, and Jiannan Tong. Application of a multifunction solar heat pump system in residential buildings. Application of a multi-function solar-heat pump system in residential buildings, 130:922–937, 2018.

[11] Alejandro Del Amo, Amaya Mart´ınez-Gracia, Angel A. Bayod-R´ujula, and Marta Ca˜nada. Performance analysis and experimental validation of a solar-assisted heat pump fed by photovoltaic-thermal collectors. Energy, 169:1214–1223, 2019.

[12] Jinzhi Zhou, Xudong Zhao, Yanping Yuan, Jing Li, Min Yu, and Yi Fan. Operational performance of a novel heat pump coupled with mini-channel pv/t and thermal panel in low solar radiation. Energyand Built Environment, 1(1):50–59, 2020.

[13] Lei Liu, Wenjie Liu, Jian Yao, Teng Jia, Yao Zhao and Yanjun Dai. Life cycle energy, economic and environmental analysis for the direct-expansion photovoltaic-thermal heat pump system in china. Journal of Cleaner Production, 434:139730, 2024.

[14] A.A. Ammar, K. Sopian, M.A. Alghoul, and et al. Performance study on photovoltaic/thermal solar-assisted heat pump system. Journal of Thermal Analysis and Calorimetry, 136:79–87, 2019.

[15] Mohamed R. Gomaa, Mujahed Al-Dhaifallah, Ali Alahmer, and Hegazy Rezk. Design, modeling, and experimental investigation of active water cooling concentrating photovoltaic system. Sustainability, 12(13):5392, 2020.

[16] Boyao Du, Zhenhua Quan, Longshu Hou, Yaohua Zhao, Xiaoying Lou, and Chunqing Wang. Experimental study on the performance of a photovoltaic/thermal air dual heat source direct-expansion heat pump. Applied Thermal Engineering, 188:116598, 2021.

[17] Tadakatsu Ohnaka, Yutaka Tochihara, and Yumiko Watanabe. The effects of variation in body temperature on the preferred water temperature and flow rate during showering. Ergonomics, 37(3):541–546, 1994.